



OPEN

# Negative Quantum Capacitance Induced by Midgap States in Single-layer Graphene

Lin Wang<sup>1\*</sup>, Yang Wang<sup>1\*</sup>, Xiaolong Chen<sup>1\*</sup>, Wei Zhu<sup>2</sup>, Chao Zhu<sup>1</sup>, Zefei Wu<sup>1</sup>, Yu Han<sup>1</sup>, Mingwei Zhang<sup>1</sup>, Wei Li<sup>1</sup>, Yuheng He<sup>1</sup>, Wei Xiong<sup>1</sup>, Kam Tuen Law<sup>1</sup>, Dangsheng Su<sup>3</sup> & Ning Wang<sup>1</sup>

<sup>1</sup>Department of Physics and the William Mong Institute of Nano Science and Technology, The Hong Kong University of Science and Technology, Hong Kong, China, <sup>2</sup>Department of Physics and Astronomy, California State University, Northridge, California 91330, USA, <sup>3</sup>Shenyang National Laboratory for Materials Science, Institute of Metal Research, Chinese Academy of Sciences, Shenyang, China.

Received  
3 May 2013

Accepted  
28 May 2013

Published  
20 June 2013

Correspondence and requests for materials should be addressed to N.W. (phwang@ust.hk)

\* These authors contributed equally to this work.

We demonstrate that single-layer graphene (SLG) decorated with a high density of Ag adatoms displays the unconventional phenomenon of negative quantum capacitance. The Ag adatoms act as resonant impurities and form nearly dispersionless resonant impurity bands near the charge neutrality point (CNP). Resonant impurities quench the kinetic energy and drive the electrons to the Coulomb energy dominated regime with negative compressibility. In the absence of a magnetic field, negative quantum capacitance is observed near the CNP. In the quantum Hall regime, negative quantum capacitance behavior at several Landau level positions is displayed, which is associated with the quenching of kinetic energy by the formation of Landau levels. The negative quantum capacitance effect near the CNP is further enhanced in the presence of Landau levels due to the magnetic-field-enhanced Coulomb interactions.

Quantum capacitance and compressibility are critical quantities reflecting the fundamental physics of electron-electron (e-e) interactions<sup>1-3</sup>. The compressibility of two-dimensional electron gas systems can have a negative sign when the influence of e-e interactions on the density of states (DOS) is drastic, in particular in the samples having very low electron density  $n$  and being subjected to a high magnetic field  $B^{4,5}$ . But single-layer graphene (SLG), a truly two-dimensional structure with a honeycomb lattice and a linear energy spectrum near the intersection of the electron and hole cones in its band structure<sup>6-9</sup>, exhibits very weak e-e interaction behavior. The single-electron model is usually sufficient to describe the electron behavior in SLG. The weak e-e interactions in SLG are mainly due to the exchange and correlation energies<sup>7</sup> cancelling each other out<sup>10,11</sup>, resulting in a positive exchange self-energy according to renormalization group theory<sup>12-14</sup>. Therefore, the inverse quantum capacitance (or inverse compressibility) is only modified by a small positive logarithmic correction in comparison with the one that ignores the e-e interactions<sup>12</sup>. Recently, G. L. Yu *et al.* reported that in high-quality pristine graphene samples, negative quantum capacitance phenomenon can be observed at half filling factors due to many-body effects under strong magnetic fields<sup>15</sup>. However, the negative quantum capacitance phenomenon in disordered graphene remains unexplored.

Unlike the experiment carried out by G.L. Yu *et al.* in which the kinetic energy is suppressed due to the formation of Landau levels, in this work, we show the first experimental evidence of reaching the strongly correlated electron regime induced by nearly dispersionless impurity bands in graphene, in the absence of a magnetic field. SLG decorated with a high density of Ag adatoms shows the unconventional phenomenon of negative quantum capacitance even in the absence of a magnetic field. This phenomenon is enhanced as the strength of the magnetic field increases. We believe that the midgap states induced by a high density of Ag adatoms deposited on SLG are responsible for this interesting experimental observation. The varied energy dispersion relationship as well as the emergence of nearly dispersionless impurity bands near the zero Fermi energy<sup>16-18</sup> leads to the suppression of the kinetic energy of electrons and the significant changes of Coulomb interactions in Ag-adsorbed SLG, particularly in the presence of a magnetic field. The capacitance measurements at different temperatures and under different strength of a magnetic field clearly demonstrate that the Coulomb interaction and Landau level (LL) quantization have a strong influence over the negative quantum capacitance phenomenon.

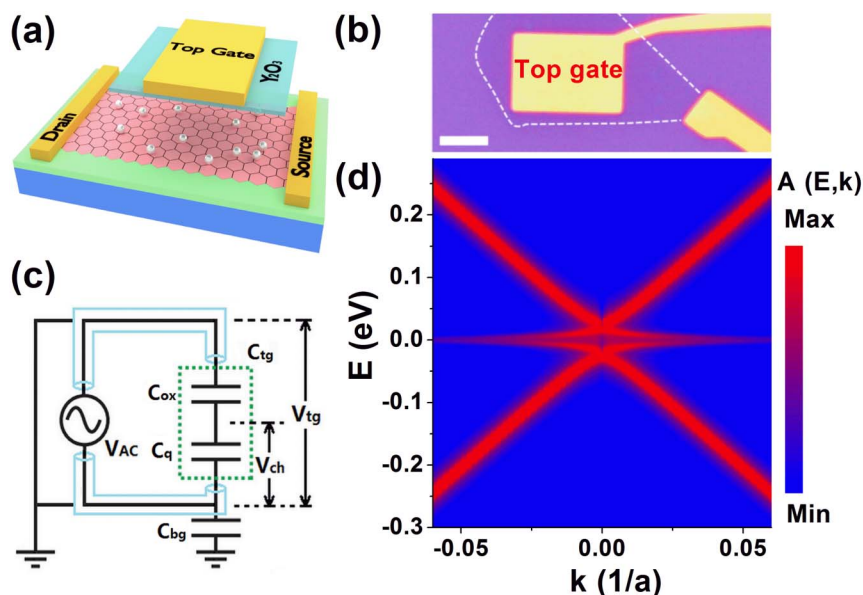


**Figure 1** | (a) Schematic diagram of the Ag-adsorbed single-layer graphene capacitor. (b) An optical image of the Ag-adsorbed single-layer graphene capacitor device; dashed line represents the graphene flake and the scale bar is 5 μm. (c) Circuit diagram of the capacitance measurements of Y<sub>2</sub>O<sub>3</sub> top-gated graphene devices. (d) Density plot of spectral function A(E,k) in k – E plane for impurity concentration  $n_i = 1\%$ , where  $a = 0.142$  nm is the nearest-neighbor distance.

## Results

Figure 1(a) schematically shows the SiO<sub>2</sub>/Ag-adsorbed graphene/Y<sub>2</sub>O<sub>3</sub> sandwiched capacitor and an optical image of one of our devices is revealed in Figure 1(b). The total capacitance  $C_{tg}$  consisting of the oxide layer capacitance  $C_{ox}$  and graphene quantum capacitance  $C_q$  in a serial configuration is shown in Figure 1(c) (see details in *Methods*). Our tight-binding calculations for SLG decorated with a high density of Ag adatoms (the impurity concentration  $n_i = 1\%$ ) show several resonant impurity bands as well as a dispersionless band near the Fermi energy  $E_F = 0$  (see Figure 1(d))<sup>19</sup>. Obviously, these changes in the quasi-particle band structure of Ag-adsorbed graphene lead to a different low-energy excitation spectrum, and thus produce midgap states (instead of the vanishing DOS in pristine SLG) in the vicinity of the charge neutrality point (CNP)<sup>16,17,19–22</sup>. Quantum capacitance (directly proportional to graphene DOS) measurements provide an effective method to probe the midgap states in graphene. As shown in Figure 2(a), a robust peak was detected when measuring the total capacitance  $C_{tg}$  versus the applied top gate voltage  $V_{tg}$  of our Ag-adsorbed SLG samples at  $T = 2$  K, confirming that Ag adatoms act as resonant impurities and create obvious midgap states near the CNP<sup>18,21,23–25</sup>.

The quantum capacitance  $C_q$  of graphene can be calculated from  $C_q^{-1} = C_{tg}^{-1} - C_{ox}^{-1}$ <sup>26–29</sup>. The oxide layer capacitance  $C_{ox}$  was obtained by measuring the internal reference parallel-plate capacitors (Au/Y<sub>2</sub>O<sub>3</sub>/Au), of which the Y<sub>2</sub>O<sub>3</sub> layers were prepared under the same experimental conditions as those for the SLG quantum capacitors<sup>27–29</sup>. Surprisingly, the values of  $C_{tg}$  in the energy region near the CNP where the robust midgap state peak appears always exceed that of the oxide layer capacitance  $C_{ox}$ , a very clear sign of negative quantum capacitance  $C_q$ <sup>15</sup>. In Figure 2(a), the dashed line denotes the value of  $C_{ox} = 0.65$  μF/cm<sup>2</sup> measured at temperature  $T = 2$  K and thus  $C_q$  is negative in the region above the dashed line. The midgap states induced by Ag adatoms obviously play a critical role in the formation of the negative quantum capacitance.

The variation in the chemical potential  $\mu$  (equivalent to the Fermi energy  $E_F$ ) as a function of top gate voltage  $V_{tg}$  can be calculated from the integral form of the charge conservation relation  $\mu = e \int_0^{V_{tg}} \left(1 - \frac{C_{tg}}{C_{ox}}\right) dV_{tg}$ <sup>27,30,31</sup>, where  $e$  is the elementary charge and the capacitance data are measured at  $T = 2$  K. The result is shown in Figure 2(b). Unlike in pristine SLG, an abnormal decline in the curve of  $\mu$  versus  $V_{tg}$  occurs in the Ag-adsorbed SLG near  $\mu = 0$ . The fact

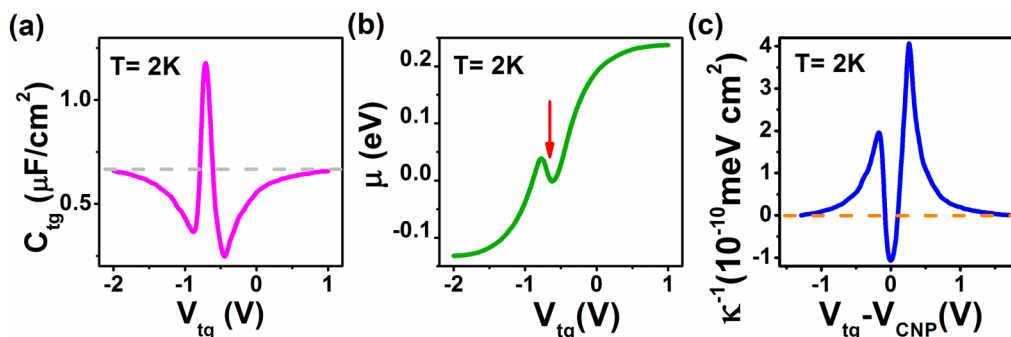


**Figure 2** | (a) Curve of the total capacitance  $C_{tg}$  versus top gate voltage  $V_{tg}$  of the Ag-adsorbed single-layer graphene capacitor measured at  $T = 2$  K where the gray dashed line denotes the value of  $C_{ox} = 0.65$  μF/cm<sup>2</sup>. (b) The relationship between chemical potential  $\mu$  versus top gate  $V_{tg}$  obtained from the data shown in Figure 2(a), where the red arrow denotes the abnormal decline of  $\kappa^{-1}$  versus  $V_{tg}$ . (c) Inverse compressibility  $\kappa^{-1}$  of Ag-adsorbed graphene measured at  $T = 2$  K where the orange dashed line denotes the zero value of  $\kappa^{-1}$ .

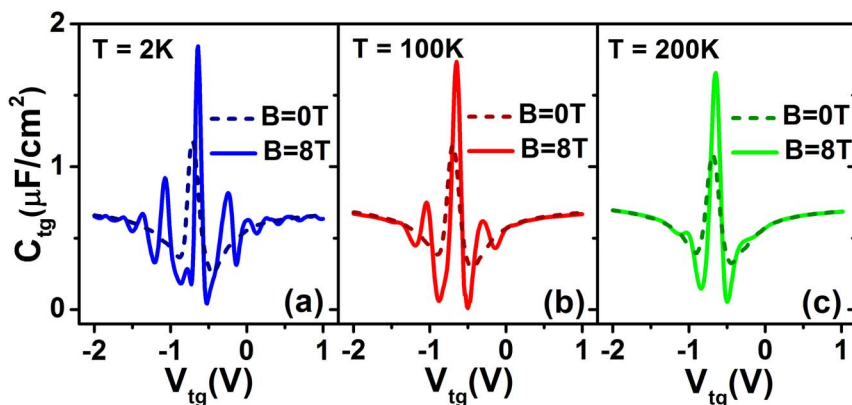


**Figure 3** | Magneto-capacitance  $C_{tg}$  measured at  $B = 8$  T versus top gate voltage  $V_{tg}$  of the Ag-adsorbed single-layer graphene capacitor obtained at (a)  $T = 2$  K (blue line), (b)  $T = 100$  K (red line) and (c)  $T = 200$  K (green line); the results measured at  $B = 0$  T (dashed lines) are shown here for comparison.

that the total energy decreases when more electrons are introduced to the sample by increasing the top gate voltage  $V_{tg}$ , implies that the energy of the incoming electrons in the region of midgap states is negative.

### Discussion

The chemical potential  $\mu$  of the electrons in SLG consists of the kinetic energy of  $E_k$  and the Coulomb interaction energy among electrons  $E_c$ , and can be denoted by  $\mu = E_k + E_c$ <sup>1,3,11,13</sup>. As the tight-binding results shown in Figure 1 (d), in low carrier density regions, the electron states would be first filled within the nearly dispersionless bands and thus the kinetic energy  $E_k$  is quenched. In this case, the Coulomb interaction energy  $E_c$  becomes dominant. The Coulomb interaction energy  $E_c$  can also vary dramatically as a consequence of the formation of midgap states. The inverse compressibility  $\kappa^{-1}$ , defined as the derivative of chemical potential  $\mu$  with respect to carrier density  $n$ ,  $\kappa^{-1} = \frac{\partial \mu}{\partial n} = \frac{\partial E_k}{\partial n} + \frac{\partial E_c}{\partial n}$ , is also determined by the kinetic energy  $E_k$  and the Coulomb energy  $E_c$ <sup>1,12,13</sup>. The experimental values of  $\kappa^{-1}$  can be obtained by  $\kappa^{-1} = e^2 C_q^{-1} = e^2 (C_{tg}^{-1} - C_{ox}^{-1})$ , as shown in Figure 2 (c). In previous theoretical studies, it has been suggested that midgap states enhance the

Coulomb interactions and the correction term induced by midgap states has a negative sign, leading to the reduction of  $\kappa^{-1}$ . The expression of  $\kappa^{-1}$  affected by midgap states is represented as<sup>1,32–34</sup>

$$\kappa^{-1} = v_F \sqrt{\frac{\pi}{4n}} \left( 1 - c \Delta \ln \frac{\Lambda}{|k|} \right) \quad (1)$$

where  $c$  is a positive numerical constant,  $\Delta$  is a positive dimensionless number characterizing the strength of midgap states and  $\Lambda$  is a high momentum cutoff of the order of the inverse of the lattice constant. Note that the second term in the bracket arising from the midgap states correction is negative and becomes significant if wave vector  $k$  is very small. Thus the experimental observation of negative compressibility or negative quantum capacitance in Ag-adsorbed SLG can be naturally understood by the fact that the midgap states lead to a negative correction of  $\kappa^{-1}$ .

The magneto-capacitance measurements for the Ag-adsorbed SLG further support a correlation between the midgap states and graphene negative quantum capacitance, particularly in the presence of LL quantization. As shown in Figure 3,  $C_{tg}$  oscillates (against top gate voltage  $V_{tg}$ ) due to LL quantization under a strong magnetic field of  $B = 8$  T at  $T = 2$  K<sup>35</sup>. Because of the thermal-activated fluctuation of carrier density  $n$ , the LLs broaden when temperature

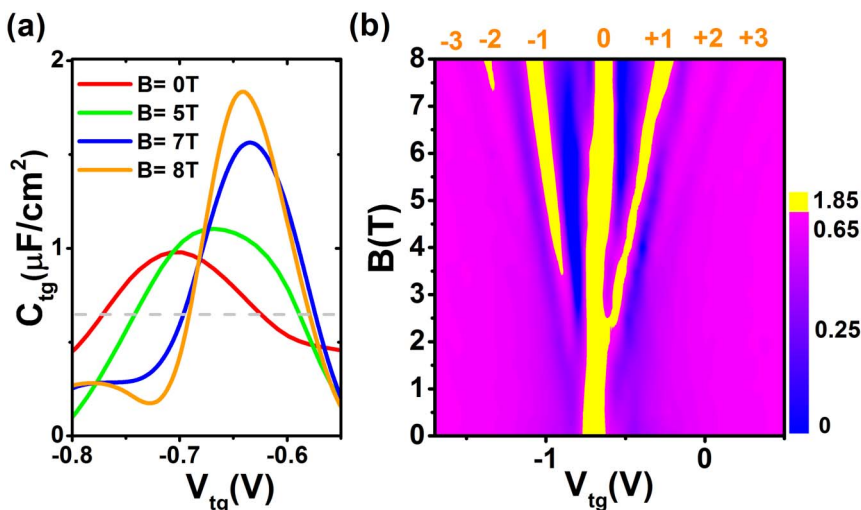


**Figure 4** | (a) Total capacitance  $C_{tg}$  versus top gate voltage  $V_{tg}$  of the Ag-adsorbed single-layer graphene capacitor measured near the CNP at  $B = 0$  T (red line),  $B = 5$  T (green line),  $B = 7$  T (blue line), and  $B = 8$  T (orange line). The gray dashed line denotes the value of  $C_{ox} = 0.65$   $\mu\text{F}/\text{cm}^2$ . (b) Two-dimensional mapping of  $C_{tg}$  measured at  $T = 2$  K as a function of top gate voltage  $V_{tg}$  and magnetic field  $B$ , where the regions in which the negative quantum capacitance (i.e.  $C_{tg} > C_{ox} = 0.65$   $\mu\text{F}/\text{cm}^2$ ) emerges are colored in yellow and the numbers above the figure denote the LL positions.



increases<sup>29,35,36</sup>. At 200 K, LLs at  $N = 0, \pm 1$  are still recognizable, while the other LLs are smeared. At  $B = 8$  T and  $T = 2$  K, the quantum capacitances measured at LL positions of  $N = \pm 1$  and  $N = -2$  where the midgap states have less overlap with the LLs also become negative. The signatures of negative capacitance at these LL locations disappear gradually as temperature increases to 200 K. The temperature dependence of the negative quantum capacitance  $C_q$  at LL positions of  $N = \pm 1$  and  $N = -2$  obviously reflects the high correlation of the degree of LL quantization with the negative  $C_q$  phenomenon. This phenomenon can be explained qualitatively by the fact that a strong magnetic field can effectively quench the kinetic energy  $E_k$  of electrons due to LL quantization, and thus the negative Coulomb energy dominates and leads to the negative  $C_q$ <sup>15,37</sup>.

Near the CNP, the midgap states and the LL at  $N = 0$  overlap forming the “central peak” of the negative  $C_q$ . The intensity of this central peak is not sensitive to temperature, unlike the behavior of other LLs as shown in Figures 3 (a)–(c). These experimental results indicate that the  $E_k$  of electrons near the CNP in Ag-adsorbed SLG has been effectively suppressed due to the formation of the dispersionless impurity band at  $E_F = 0$ . In this case, the magnetic quenching effect on the  $E_k$  attributed to the  $N = 0$  LL is insignificant and we can observe very obvious negative  $C_q$  phenomenon near CNP even in the absence of magnetic field. However, we do observe that the negative  $C_q$  is very sensitive to the variation in a magnetic field (see Figure 4 (a)). Since the complete quenching effect on  $E_k$  near  $E_F = 0$  occurs with or without a magnetic field (based on the above analysis), we ascribe the magnetic-field-enhanced negative  $C_q$  effect near the CNP to the contribution of the Coulomb interaction energy  $E_C$ , which has been greatly altered due to the presence of a magnetic field in our samples. Under a magnetic field, electronic motion in SLG is localized and a huge population induced by the formation of zero LL leads to a massive degeneracy near CNP<sup>7</sup>. Thus the Coulomb interaction energy should increase and the negative  $C_q$  will be enhanced, as the magnetic field becomes stronger.

The variation in  $C_{tg}$  as a function of  $B$  and  $V_{tg}$  measured at  $T = 2$  K is revealed in Figure 4 (b). The general features of the LLs (particularly the high energy LLs) for the Ag-adsorbed SLG follow the prediction of LL quantization theory for pristine SLG. The regions colored in yellow indicate the negative  $C_q$  regions, which start to emerge at the  $N = \pm 1$  LLs as  $B$  increases to  $2 \sim 3$  T. This is very different from the weak negative  $C_q$  observed in high-quality pristine SLG under a strong magnetic field  $B = 5 \sim 25$  T<sup>15</sup>. We believe that weak resonant impurity bands exist at some distance away from  $E_F = 0$ . The midgap states induced by resonant impurities should also influence the electrons located at some distance away from the CNP (e.g., at the  $N = \pm 1$  LLs), although their effects on negative  $C_q$  are not as strong as those of the midgap states that are close to the CNP. Therefore, the negative  $C_q$  in the presence of a magnetic field in Ag-adsorbed SLG should mainly incorporate the effects from the suppression of  $E_k$  and the enhancement of  $E_C$ , both of which are directly correlated with magnetic fields and various resonant impurity bands.

In summary, we find that the novel phenomenon of negative quantum capacitance observed in single-layer graphene decorated with a high density of Ag adatoms is attributed to the midgap states induced by the resonant impurities of the Ag adatoms. Owing to these Ag-induced midgap states, the kinetic energy of the electrons near the zero Fermi energy is effectively quenched and the Coulomb interaction energy is varied dramatically, and the combination of these two events leads to the abnormal negative quantum capacitance of the “central peak” in the absence of a magnetic field. In the presence of a magnetic field, the negative quantum capacitance is dramatically enhanced. The emergence of the negative quantum capacitance away from the CNP is intimately associated with the degree of Landau level quantization, while the magnetic-field-enhanced Coulomb interactions give rise to the increase of negative quantum capacitance near the CNP with the magnetic fields.

## Methods

Single-layer graphene (SLG) samples were prepared by the micromechanical exfoliation of Kish graphite and placed on silicon substrates with 300 nm-thick  $\text{SiO}_2$ . Raman spectroscopy has been used to identify these samples as single-layer graphene. Ag adatoms were introduced to SLG by DC plasma sputtering in high base vacuum conditions ( $10^{-7}$  torr) at room temperature<sup>38,39</sup>. An ultrathin yttrium layer (5 nm in thickness) was deposited on the Ag-adsorbed SLG by e-beam evaporation and then the SLG was oxidized in air at 180°C for 30 minutes<sup>27,29</sup>. The fabrication of drain/source and top gate electrodes (Ti/Au = 5/40 nm) was performed by conventional electron-beam lithography techniques (Raith e-Line Nanoengineering Workstation and AST electron-beam evaporation system)<sup>38,39</sup>. As shown in Figure 1, the total capacitance  $C_{tg}$  in a series of the oxide layer capacitance  $C_{ox}$  and graphene quantum capacitance  $C_q$  was measured by an integrated capacitance bridge for high sensitivity. This capacitance bridge delivered extremely high resolution of atto farad (aF) under very small excitation ( $\sim 0.1$  mV) driving any possible parasitic capacitance by a high mobility electron transistor (HMET)<sup>26,27,35,38,40,41</sup>.

- Kotov, V. N., Uchoa, B., Pereira, V. M., Guinea, F. & Castro Neto, A. H. Electron-Photon Interactions in Graphene: Current Status and Perspectives. *Reviews of Modern Physics* **84**, 1067–1125 (2012).
- Abergel, D. S. L., Hwang, E. H. & Das Sarma, S. Compressibility of graphene. *Physical Review B* **83**, 085429 (2011).
- Martin, J. *et al.* Observation of electron-hole puddles in graphene using a scanning single-electron transistor. *Nature Physics* **4**, 144–148 (2008).
- Eisenstein, J. P., Pfeiffer, L. N. & West, K. W. Negative compressibility of interacting two-dimensional electron and quasiparticle gases. *Physical Review Letters* **68**, 674–677 (1992).
- Eisenstein, J. P., Pfeiffer, L. N. & West, K. W. Compressibility of the two-dimensional electron gas: Measurements of the zero-field exchange energy and fractional quantum Hall gap. *Physical Review B* **50**, 1760–1778 (1994).
- Novoselov, K. S. *et al.* Two-dimensional gas of massless Dirac fermions in graphene. *Nature* **438**, 197–200 (2005).
- Castro Neto, A. H., Guinea, F., Peres, N. M. R., Novoselov, K. S. & Geim, A. K. The electronic properties of graphene. *Reviews of Modern Physics* **81**, 109–162 (2009).
- Peres, N. M. R. Colloquium: The transport properties of graphene: An introduction. *Reviews of Modern Physics* **82**, 2673–2700 (2010).
- Das Sarma, S., Adam, S., Hwang, E. H. & Rossi, E. Electronic transport in two-dimensional graphene. *Reviews of Modern Physics* **83**, 407–470 (2011).
- Peres, N. M. R., Guinea, F. & Castro Neto, A. H. Coulomb interactions and ferromagnetism in pure and doped graphene. *Physical Review B* **72**, 174406 (2005).
- Barlas, Y., Pereg-Barnea, T., Polini, M., Asgari, R. & MacDonald, A. H. Chirality and Correlations in Graphene. *Physical Review Letters* **98**, 236601 (2007).
- Sheehy, D. E. & Schmalian, J. Quantum Critical Scaling in Graphene. *Physical Review Letters* **99**, 226803 (2007).
- Hwang, E. H., Hu, B. Y.-K. & Das Sarma, S. Density Dependent Exchange Contribution to  $\partial\mu/\partial n$  and Compressibility in Graphene. *Physical Review Letters* **99**, 226801 (2007).
- Shankar, R. Renormalization-group approach to interacting fermions. *Reviews of Modern Physics* **66**, 129–192 (1994).
- Yu, G. L. *et al.* Interaction phenomena in graphene seen through quantum capacitance. *Proceedings of the National Academy of Sciences of the United States of America* **110**, 3282–3286 (2013).
- Wehling, T. O., Katsnelson, M. I. & Lichtenstein, A. I. Adsorbates on graphene: Impurity states and electron scattering. *Chemical Physics Letters* **476**, 125–134 (2009).
- Wehling, T. O., Katsnelson, M. I. & Lichtenstein, A. I. Impurities on graphene: Midgap states and migration barriers. *Physical Review B* **80**, 085428 (2009).
- Yuan, S. J., De Raedt, H. & Katsnelson, M. I. Modeling electronic structure and transport properties of graphene with resonant scattering centers. *Physical Review B* **82**, 115448 (2010).
- Zhu, W. *et al.* Vacancy-induced splitting of the Dirac nodal point in graphene. *Physical Review B* **85**, 073407 (2012).
- Pereira, V. M., Guinea, F., Lopes dos Santos, J. M. B., Peres, N. M. R. & Castro Neto, A. H. Disorder Induced Localized States in Graphene. *Physical Review Letters* **96**, 036801 (2006).
- Stauber, T., Peres, N. M. R. & Guinea, F. Electronic transport in graphene: A semiclassical approach including midgap states. *Physical Review B* **76**, 205423 (2007).
- Robinson, J. P., Schomerus, H., Oroszlány, L. & Fal’ko, V. I. Adsorbate-Limited Conductivity of Graphene. *Physical Review Letters* **101**, 196803 (2008).
- Liu, X. J. *et al.* Bonding and charge transfer by metal adatom adsorption on graphene. *Physical Review B* **83**, 235411 (2011).
- Wehling, T. O., Katsnelson, M. I. & Lichtenstein, A. I. Impurities on graphene: Midgap states and migration barriers. *Physical Review B* **80**, 085428 (2009).
- Ferreira, A. *et al.* Unified description of the dc conductivity of monolayer and bilayer graphene at finite densities based on resonant scatterers. *Physical Review B* **83**, 165402 (2011).
- Xia, J. L., Chen, F., Li, J. H. & Tao, N. J. Measurement of the quantum capacitance of graphene. *Nature Nanotechnology* **4**, 505–509 (2009).



27. Xu, H. L. *et al.* Quantum Capacitance Limited Vertical Scaling of Graphene Field-Effect Transistor. *Acs Nano* **5**, 2340–2347 (2011).
28. Wang, Z. X. *et al.* Growth and Performance of Yttrium Oxide as an Ideal High-kappa Gate Dielectric for Carbon-Based Electronics. *Nano Letters* **10**, 2024–2030 (2010).
29. Wang, L. *et al.* Modification of electronic properties of top-gated graphene devices by ultrathin yttrium-oxide dielectric layers. *Nanoscale* **5**, 1116–1120 (2013).
30. Droscher, S. *et al.* Quantum capacitance and density of states of graphene. *Applied Physics Letters* **96**, 152104 (2010).
31. Xu, H. L., Zhang, Z. Y. & Peng, L. M. Measurements and microscopic model of quantum capacitance in graphene. *Applied Physics Letters* **98**, 133122 (2011).
32. Foster, M. S. & Aleiner, I. L. Graphene via large N: A renormalization group study. *Physical Review B* **77**, 195413 (2008).
33. Foster, M. S. & Ludwig, A. W. W. Metal-insulator transition in Hubbard-like models with random hopping. *Physical Review B* **74**, 241102 (2006).
34. Foster, M. S. & Ludwig, A. W. W. Interaction effects on two-dimensional fermions with random hopping. *Physical Review B* **73**, 155104 (2006).
35. Ponomarenko, L. A. *et al.* Density of States and Zero Landau Level Probed through Capacitance of Graphene. *Physical Review Letters* **105**, 136801 (2010).
36. Zhu, W. *et al.* Shape of Disorder-Broadened Landau Subbands in Graphene. *Physical Review Letters* **102**, 056803 (2009).
37. Skinner, B. & Shklovskii, B. I. Giant capacitance of a plane capacitor with a two-dimensional electron gas in a magnetic field. *Physical Review B* **87**, 035409 (2013).
38. Li, W. *et al.* Electron localization in metal-decorated graphene. *Physical Review B* **84**, 045431 (2011).
39. He, Y. H. *et al.* Modifying electronic transport properties of graphene by electron beam irradiation. *Applied Physics Letters* **99**, 033109 (2011).
40. Hazeghi, A., Sulpizio, J. A., Diankov, G., Goldhaber-Gordon, D. & Wong, H. S. P. An integrated capacitance bridge for high-resolution, wide temperature range quantum capacitance measurements. *Review of Scientific Instruments* **82**, 5 (2011).
41. Li, W. *et al.* Density of states and its local fluctuations determined by capacitance of strongly disordered graphene. *Scientific Reports* **3**, 1772 (2013).

## Acknowledgments

The authors are grateful for fruitful discussions with Professors Ping Sheng and Zhaoqing Zhang and the technical assistance of Professor Ho Bun Chan. Financial support from the Research Grants Council of Hong Kong (Project Nos. 604112, N\_HKUST613/12 and HKUST9/CRF/08) and technical support of the Raith-HKUST Nanotechnology Laboratory for the electron-beam lithography facility at MCPF (Project No. SEG\_HKUST08) are hereby acknowledged.

## Author contributions

L. Wang and Y. Wang and N. Wang wrote the main manuscript and L. Wang prepared Figures 1–4. The experimental work was mainly done by L. Wang., C. Zhu., X.L. Chen., Y. Wang and the theoretical calculations were performed by W. Zhu. All authors reviewed the manuscript.

## Additional information

**Competing financial interests:** The authors declare no competing financial interests.

**How to cite this article:** Wang, L. *et al.* Negative Quantum Capacitance Induced by Midgap States in Single-layer Graphene. *Sci. Rep.* **3**, 2041; DOI:10.1038/srep02041 (2013).



This work is licensed under a Creative Commons Attribution-NonCommercial-NoDerivs 3.0 Unported license. To view a copy of this license, visit <http://creativecommons.org/licenses/by-nc-nd/3.0>